Spectral Convolution for Quantitative Analysis in EPR Spectroscopy

Natalia A. Chumakova, Sergei V. Kuzin & Anatoly I. Grechishnikov

Applied Magnetic Resonance

ISSN 0937-9347
Volume 50
Number 9

Appl Magn Reson (2019) 50:1125-1147
DOI 10.1007/s00723-019-01133-9

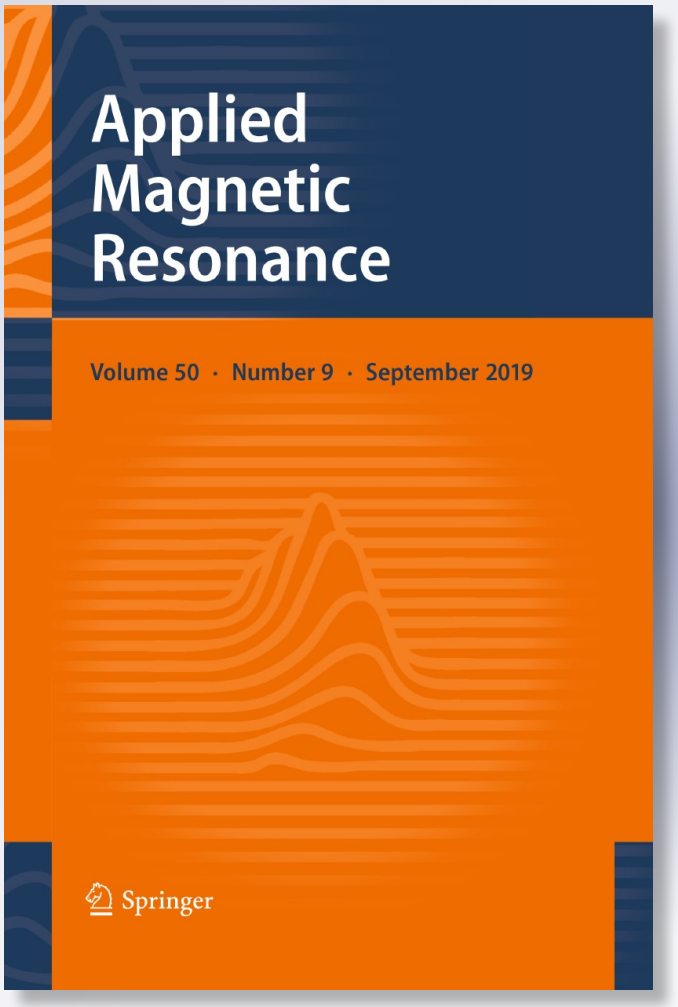

Springer

Applied Magnetic Resonance (2019) 50:1125–1147
https://doi.org/10.1007/s00723-019-01133-9

Applied
Magnetic Resonance

ORIGINAL PAPER

Spectral Convolution for Quantitative Analysis in EPR Spectroscopy

Natalia A. Chumakova[1] · Sergei V. Kuzin[1] · Anatoly I. Grechishnikov[2]

Received: 3 March 2019 / Revised: 2 May 2019 / Published online: 23 May 2019

Abstract
A method for the determination of number of spins from EPR spectra with a high level of noise is proposed. The method is based on a convolution of the experimental spectrum with the spectrum of the same shape characterized by a high signal-to-noise ratio. It was shown that the convolution technique is rather robust to the presence of additive noise in examined EPR spectrum.

1 Introduction

One of the most important procedures of the electron paramagnetic resonance (EPR) spectroscopy is the correct determination of number of paramagnetic particles in a sample followed by estimation of radical concentration in different media. Data on concentration of spin probes and spin labels are of special interest in chemistry, biology, pharmacology, etc. [1–5]. The standard method for determining the number of paramagnetic particles in a sample is based on a double integration of EPR signal. All modern EPR spectrometers are equipped with computer programs that make it possible to integrate experimental spectrum and compare the value of double integral with the standard one for determining the number/concentration of paramagnetic particles. The standard value should be obtained previously for the sample with known number of spins. Standard samples are usually supplied by manufacturer of the spectrometers, or the researcher can prepare them himself. A detailed analysis of the instrumental (Bruker's spectrophotometer is considered) and the experimental factors affecting the accuracy of measuring the absolute number of paramagnetic particles are presented in the monograph [6]. It is necessary to note that in case of highly noisy spectrum the double integration procedure cannot yield an accurate result because of difficulties in the baseline correction. In Ref. [7], it was

✉ Natalia A. Chumakova
harmonic2011@yandex.ru

[1] Chemistry Department, Lomonosov Moscow State University, Leninskiye Gory 1-3, 119991 Moscow, Russia

[2] Scientific Production Company ABION, Taganrog, Russia

shown that if the signal-to-noise ratio (SNR) is less than 20, the contribution of the integration procedure to the total error of measuring number of spins increases fast with the rise of noise.

Another possibility to determine the number of radicals in a sample is comparing the intensity of the studied spectrum with the intensity of the spectrum of another sample of the same "radical-medium" system which is characterized by high SNR and can be integrated accurately. Such spectrum is referred to here as a standard spectrum. Usually, the comparison of intensities of two spectra is made by comparing of intensities of corresponding spectral components. In such a case, only two points of experimental spectrum are used to obtain the quantitative information. Besides, the procedure of measuring amplitude of highly noisy spectrum cannot yield the accurate results.

Digital denoising of spectra can be performed before double integration or amplitude measurement. Frequency filtering using Fourier transform, various types of wavelet transforms, discrete sine and cosine transforms, Hartley transform, etc. yields good results in the cases of moderately noisy spectra. For example, the authors of [8] showed that the wavelet filtering made it possible denoising of CW-EPR spectra with SNR about 6–8 (visually estimated) with almost no distortion. However, when a spectrum is highly noisy (SNR close to one or less than one), the standard denoising procedures do not allow reliable extracting spectrum from the noise.

In this work, another approach to quantitative processing of EPR spectra which is based on a convolution with a standard spectrum is proposed. Such a procedure makes it possible to use all the points of investigated and standard spectra for receiving the quantitative information. The basic principles of such processing of highly noisy signals were formulated as the results of studies aimed at optimizing the functioning of radar systems [9, 10]. In the present work, the efficiency of application of convolution technique for obtaining quantitative information from highly noisy CW-EPR spectra was studied in series of numerical and experimental tests. Low sensitivity of the proposed method to the presence of additive white noise was demonstrated: if the signal-to-noise ratio was 1, the error in determining number of spins was found to be about 5%.

2 Results and Discussion

2.1 Basic Information

Convolution procedure [11] can be presented as follows:

$$I(B)*(B) \stackrel{\text{def}}{=} \int_{-\infty}^{+\infty} I\left(B'\right) J\left(B - B'\right) \mathrm{d}B', \tag{1}$$

where $I(B)$ and $J(B)$ are experimental and standard spectra, respectively. The entire magnetic field including both spectra must be taken as the integration limits. If the shape of standard spectrum coincides with the shape of experimental one, the maximal value of function (1) corresponds to complete spectra overlapping. The procedure of the spectra convolution is demonstrated in Fig. 1.

The convolution procedure was used in EPR spectroscopy to detect a narrow spectrum of the fast rotating radicals against the background of the broad spectrum belonging to radicals with the low rotational correlation times [12], and to determine the HFS constants in complex spectra including a large number of components [13, 14]. As far as we know, this procedure was not used previously for quantitative analysis of EPR spectra.

The convolution transforming has the following feature [11]:

$$(c \cdot I) * J = c \cdot (I * J). \tag{2}$$

The feature (2) makes it possible to receive information about number of spins in the studied sample provided the number of spins in the standard sample (N_{st}) is known. It is necessary to take into account spectra recording parameters which affect intensity of EPR signals: modulation amplitude (A), microwave power (P), amplification coefficient (R) of a signal (receiver gain) and resonator quality factor (Q). The expression for calculation of number of spins (N_{exp}) from the maximal value of convolution function (*MaxConv*) is the following:

$$N_{exp} = N_{st} \frac{A_{st}}{A_{exp}} \frac{Q_{st}}{Q_{exp}} \frac{R_{st}}{R_{exp}} \sqrt{\frac{P_{st}}{P_{exp}}} \frac{MaxConv}{MaxAutoConv}. \tag{3}$$

Herein, *MaxAutoConv* is the maximal value of convolution of standard spectrum with itself (autoconvolution). The expression (3) implies that the both standard and experimental spectra are not distorted due to inappropriate magnitude of modulation (A) as well as that of power (P). This expression comprises Q-factors which are

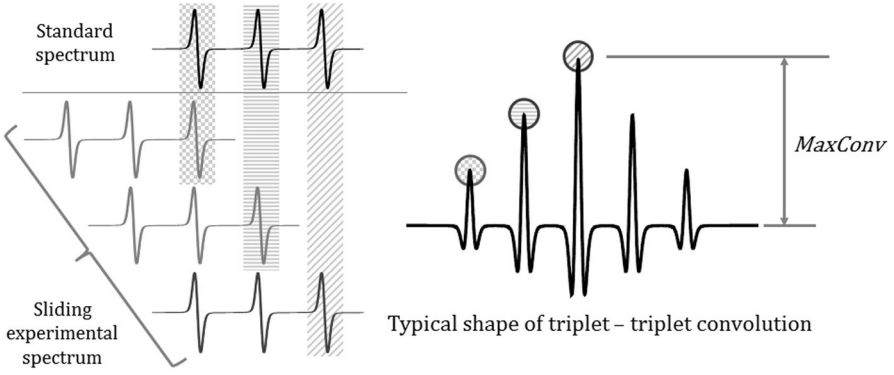

Fig. 1 Procedure of convolution for two triplet EPR spectra. Peaks in the convolution graph correspond to entire overlapping of 1, 2, 3, 2 and 1 triplet components, respectively, while the second (experimental) spectrum shifts in respect to the first one (standard). Intensity of the central peak in this paper is considered as *MaxConv*

always determined with significant errors (8–15% [7]), so the accuracy of the considered method cannot surpass that of Q-factor measurement. For correct determination of N_{st}, it is important to make spectrometer calibration using primary standards (Mn^{2+}/MgO, $CuSO_4$, DPPH, etc.). The problems accompanying the calibration procedure are discussed in detail in the works [15, 16].

As was shown [9], the signal-to-noise ratio of convolution result is much higher than that of experimental spectrum. Figure 2 presents the convolution of triplet spectrum with numerically noised one. One can see that convolution function is much smoother than experimental spectrum. Therefore, measuring of maximal amplitude of convolution function can be performed with a high accuracy.

Significant difference between the signal-to-noise ratio of experimental spectrum and its convolution with standard spectrum is the result of convolution procedure [9]. Besides, EPR signal is a typical low-frequency narrowband signal, which gives additional opportunities to increase SNR. This can be explained in terms of EPR spectra Fourier-transform (FT) images. FT images of two EPR signals and their convolution meet the convolution theorem ($\mathcal{F}$ means Fourier transform) [11]:

$$\mathcal{F}[I*J] = \sqrt{2\pi}\mathcal{F}[I] \cdot \mathcal{F}[J]. \tag{4}$$

Hence, convolution procedure means in fact the multiplication of two EPR spectra Fourier images. The Fourier image intensity $\mathcal{F}[I](\omega)$ (complex, in general) corresponding to the frequency ω reflects contribution of the oscillating function $e^{i\omega B}$ to the original EPR spectrum $I(B)$. It is clear that the proper EPR signal and noise are described by different sets of frequencies, namely noise includes the higher ones. Consequently, during the convolution procedure the intensity of experimental spectrum FT image in the range of "noise frequencies" will be multiplied by zero intensity of the standard spectrum FT image in the same range. As a result, the truncation of "noise frequencies" in FT image of convolution and, consequently, the truncation of noise in convolution function takes place. Figure 3 presents the FT images of both noiseless triplet EPR spectrum and noisy one. One can see the contribution of "noise frequencies" at the right side of FT image of the noisy spectrum.

It is necessary to note that comparison of the intensities of two spectra (experimental and standard) can be made not only by convolution technique but also by

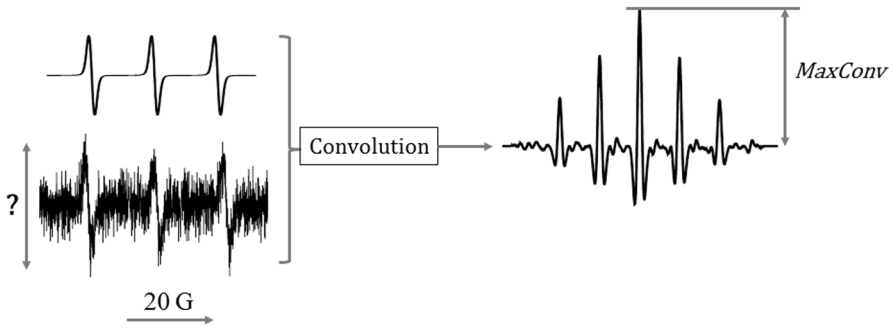

Fig. 2 Convolution of triplet EPR spectrum with numerically noised one

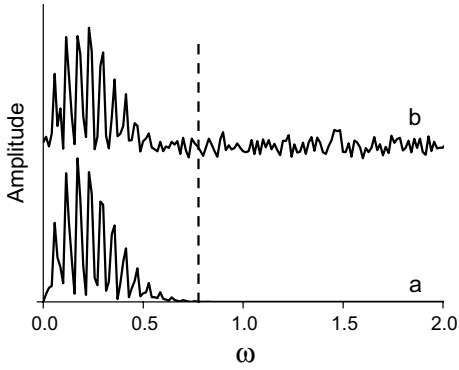

Fig. 3 Absolute intensities of Fourier-transform images for noiseless triplet EPR spectrum (a) and for the same spectrum with SNR = 2 (b). Both spectra are shown in Fig. 2

least-squares fitting of experimental spectrum. In such case, the experimental spectrum is presented as production of the standard one by a coefficient. The optimal coefficient corresponding to minimal deviations of the experimental spectrum from the scaled standard one would be equal to *MaxConv/MaxAutoConv*. It can be easily shown mathematically. The sum of the squares deviations can be presented as following:

$$U(c) = \int_{-\infty}^{\infty} \left(I_{\text{exp}}(B) - c \cdot I_{\text{st}}(B)\right)^2 \text{d}B. \tag{5}$$

The condition of the function $U(c)$ minimum is the equality to zero of its first derivative; hence,

$$c_{\text{opt}} = \frac{\int_{-\infty}^{\infty} I_{\text{exp}}(B) I_{\text{st}}(B) \text{d}B}{\int_{-\infty}^{\infty} I_{\text{st}}(B) I_{\text{st}}(B) \text{d}B} = \frac{MaxConv}{MaxAutoConv}. \tag{6}$$

Consequently, there is no need to make minimization procedure. It is enough to calculate the sum of the products of corresponding points of spectra according to the formula (6). But it is necessary earlier to shift experimental and standard spectra along magnetic field axis for complete mutual overlapping. Such a shift can be computed from the microwave frequencies of the spectra. However, the convolution technique makes it possible to compute the scale factor in automatic mode without preliminary spectra recalculation. Indeed, maximum of convolution function corresponds to complete mutual overlapping in case of absolutely noiseless experimental and standard spectra or being very close to complete mutual overlapping in case of somewhat noisy spectra. Besides, there are some cases where the convolution method can be applicable while the scaling technique is not. In 2D experiments (e.g. temperature or angular dependence of EPR spectra made by Bruker's EPR spectrometers), only the frequency of the first spectrum is put in the spectrum file. Meanwhile, it is known that the microwave frequency is changed to some extent during the experiment. To apply the least-squares fitting, one should manually fix

the working frequency of every spectrum in the series. In contrast, the convolution technique provides fast and accurate processing of large spectral series in automatic mode.

It is necessary to discuss in more detail the procedure of obtaining standard spectrum for the studied system "radical–medium". It is clear that the optimal filter is the absolutely noiseless spectrum, the shape of which coincides with the shape of experimental spectrum. Such optimal filter can be obtained by computer calculation. In case, when all magnetic and relaxation characteristics of the "radical–medium" system are exactly known, standard spectrum can be calculated using EasySpin software package or using the programs described in articles [17, 18] which make it possible to calculate the EPR spectra in rigid limit or slow motion regime, respectively. If the required parameters are unknown, it is possible to fit the experimentally recorded spectrum of the considered system "radical–medium". Note that not every EPR spectrum can be fitted correctly. For example, the simulation model can be too complicated for the EPR spectra of spin probes located in polymer matrixes. It is known that such spin probes are characterized by broad distribution of their rotational mobility [19, 20]. As is also known, the EPR spectra of paramagnetic molecules in non-viscous fluids can be distorted due to the Heisenberg exchange interaction [21]. If some parameters of the standard spectrum cannot be obtained unequivocally, one can perform the convolution of experimental spectrum with the set of calculated spectra which differ in these parameters. The maximum value of the *MaxConv* means the best match of calculated spectrum with the experimental one. Such approach is known as the adaptive filtering [10]. It can be applied to analysis of EPR spectrum which is the superposition of several spectra of paramagnetic particles. In such a case, the variable parameters are the contributions of individual components to the mixture.

In some cases, one can use the sub-optimal filter—experimental spectrum of the considered "radical–medium" system including low-amplitude noise. There are several possibilities to obtain such a standard spectrum. The first one is multiple spectrum accumulation, which leads to SNR reduction as the square root of accumulation number [6]. In case of spectra with a high level of noise, the procedure of accumulation takes considerable time. Moreover, as it was mentioned above, the frequency of electromagnetic radiation in modern EPR spectrometers cannot be kept constant for a long time. Therefore, the accumulation procedure performed in automatic mode can lead to some spectral distortion. To avoid this effect, it is necessary to make the procedure in manual mode, that comprises recording spectra and determining the radiation frequency for each of them, recalculation of all spectra to unique frequency/wavelength and subsequent averaging the obtained spectra. The second way to obtain the standard spectrum is to perform denoising of experimental spectrum by means of "noise frequencies" truncation (for example, [8]). The truncation procedure should be performed under visual control to avoid the spectrum distortion, especially, if the spectrum consists of very narrow lines described by high frequencies in the "noise frequencies" region.

The third and the easiest way of receiving a standard spectrum is to prepare the sample of the considered "radical–medium" system with a higher concentration of paramagnetic substance compared with analyzed samples. The spectrum of a highly

concentrated sample can be recorded with a good quality. As shown below, the low-amplitude noise in a standard spectrum does not affect considerably the result of convolution procedure. However, such an approach involves some difficulties. First, the standard spectrum can have wider lines compared with the experimental because of dependence of spectral line width upon concentration of radicals. The concentration broadening the lines of EPR spectra is caused by dipole–dipole interaction of radicals and the Heisenberg spin exchange [22, 23]. Second, the distance between the spectral components can be changed as a result of spin exchange interaction [22]. In cases above, the shape of standard spectrum does not reproduce exactly the shape of experimental spectrum; therefore, the *MaxConv* value deviates from its true value. As shown later, the influence of the described distortions of standard spectrum on the result of convolution procedure can be taken into consideration analytically.

2.2 Numerical Tests

2.2.1 Test 1: The Influence of Noisiness of Experimental Spectra

To determine the extent of influence of noise level of experimental spectrum on accuracy in defining the maximal convolution amplitude, the following numerical test was performed. The triplet EPR spectrum (three identical Gaussian lines, $a = 17$ G, $\Delta B_{pp} = 1.5$ G) was theoretically calculated and then artificially noised to various extent. The normally distributed noise was chosen (computational details). SNR was defined as EPR spectrum amplitude divided by 2σ, where σ is the standard deviation of noise. The intensity in every point of experimental spectrum is the sum of the true spectrum value and random noise:

$$I_{exp}(B) = I_{ESR}(B) + I_{noise}(B). \tag{7}$$

The second summand, unpredictable and stochastic part of the spectrum, is called in this paper "the noise scattering along the spectrum". In such a case, each and every spectrum is characterized by unique noise scattering. Therefore, two consecutively recorded noisy spectra of the same sample are the different functions from mathematical point of view. Thus, they yield the different results while processing. Taking into consideration above, the initial spectrum was independently randomly noised by 2000 times for every level of noise. The convolution function of each noisy spectrum with the initial noiseless spectrum was calculated and its maximum intensity (*MaxConv*) was measured automatically. To assess the noise influence on accuracy of *MaxConv* determining, we used the parameter $Dev = MaxConv/MaxConv_0 - 1$, the relative deviation of *MaxConv* from the maximal value of convolution function of the noiseless spectrum with itself ($MaxConv_0$). As expected, the *Dev* value depends on the noise level of analyzed spectra. Moreover, it was revealed that this value also depends on the noise scattering to some extent. This phenomenon is considered in detail in Appendix 1. The results corresponding to the equal level of noise but with different noise scattering along the spectrum were statistically processed. The average value and dispersion of *Dev* value were calculated. The results

Table 1 Relative deviations of *MaxConv* from $MaxConv_0$ (see text) for different levels of noise in standard and experimental spectra

SNR(exp)	Noiseless standard		SNR(st) = 20		SNR(st) = 10		SNR(st) = 5	
	Average	Dispersion	Average	Dispersion	Average	Dispersion	Average	Dispersion
20.0	− 0.01	0.26	− 1.39	0.36	− 5.34	0.56	− 18.36	0.83
5.0	− 0.05	1.08	− 1.40	1.07	− 5.20	1.17	− 18.07	1.29
3.3	0.03	1.57	− 1.27	1.62	− 5.18	1.69	− 17.89	1.75
2.5	− 0.05	2.04	− 1.27	2.11	− 4.94	2.17	− 17.56	2.21
2.0	0.03	2.68	− 1.14	2.64	− 4.85	2.72	− 17.39	2.72
1.0	0.13	5.13	− 0.96	5.10	− 4.07	5.21	− 15.86	5.23
0.5	0.82	10.28	0.37	10.50	− 2.21	10.72	− 12.34	10.11

For each noise level, the statistical processing was made by 2000 generations of noise. Dispersion in %

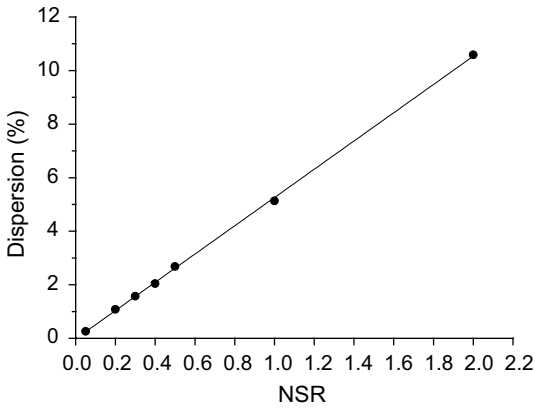

Fig. 4 Dependence of *MaxConv* dispersion on the noise-to-signal ratio

of calculations are represented in Table 1. As can be seen, if SNR is more than 2, the average values of *Dev* are close to zero. In case of lower SNR, they shift to the positive region due to the automatic procedure of *MaxConv* measurement. It was revealed that the dispersion of relative deviation of *MaxConv* measured in % depends linearly on the noise-to-signal ratio with the slope close to 5 (Fig. 4). The dispersion can be considered as the expected error of *MaxConv* in a real experiment. But the result of the single spectrum processing can differ from this value (for details, Appendix 1). For example, if the signal-to-noise ratio is 0.5 (signal is covered by noise), the expected error is ~ 11% and the maximum one is about 33%. This means that even in case of very high noise level, it is possible to estimate the number of paramagnetic molecules in the sample using the convolution technique.

2.2.2 Test 2: The Influence of Noisiness of Standard Spectrum

Standard spectra obtained in experiments always contain some noise. In case of slow solubility of paramagnetic substance in the considered solvent, the standard spectrum will be characterized by not very high SNR (< 20). This case was

considered numerically and the results are presented in Table 1. The same procedures, as described above, were made but the noised spectrum (with SNR 20, 10 and 5) was taken as a standard. It was found that noise increasing in standard spectrum increases the underestimation of number of spins determined by convolution technique; meanwhile, the dispersion is kept almost constant. Trend to decreasing the number of spins can be explained by significant increase of denominator in Eq. 3, i.e. *MaxAutoConv*. This value is the result of integration of $I_{st}(B)^2$. If $I_{st}(B)$ has the noise contribution, its squared value is severely positive in the region between and beyond triplet components, so the integral value will be overestimated. To avoid this systematic error, the standard spectrum should be as noiseless as possible. However, note that in the case of a rather noisy standard spectrum ($SNR_{st} = 10$) and a highly noisy experimental ($SNR_{exp} = 1$) one, the *MaxConv* relative deviations from *MaxConv*$_0$ are less than 5%, i.e. less than an error Q value determination.

2.2.3 Test 3: The Influence of Broadening of the Standard Spectrum

If EPR spectrum of the studied system consists of one or several well-resolved components, and it is possible to determine shape and line width of corresponding components of experimental and standard spectra, the exact expression that reflects dependence of *MaxConv* from the standard spectrum broadening can be deduced. The line shape is commonly described by Gaussian (G) or Lorentzian (L) functions or their convolution (called the Voigt profile) (V). According to the convolution theorem, FT image of convolution of two Gauss (Lorentz, Voigt) functions can be calculated from FT images of each function. For example, in case of Gaussian:

$$\mathcal{F}\left[G_{exp} * G_{st}\right] = \sqrt{2\pi}\mathcal{F}\left[G_{exp}\right] \cdot \mathcal{F}\left[G_{st}\right]. \tag{8}$$

Here, G_{st} and G_{exp} are the Gauss functions describing standard and experimental spectra, correspondingly. The Gaussian and Lorentzian lines in EPR are described as follows (center of the lines is at $B_0 = 0$) [1]:

$$G(B) = -\frac{I}{\sqrt{2\pi}\sigma^3} B \exp\left(-\frac{B^2}{2\sigma^2}\right), \tag{9a}$$

$$L(B) = -\frac{2I}{\pi} \frac{\sqrt{3}\sigma B}{\left(3\sigma^2 + B^2\right)^2}. \tag{9b}$$

Here, B is magnetic field, $\sigma = \Delta B_{pp}/2$, and ΔB_{pp} is peak-to-peak width of the EPR spectral line (the distance between the maximum inclination points in absorbance spectrum). FT images of Gaussian and Lorentzian profiles are the following:

$$\mathcal{F}[G] = \frac{i\omega}{\sqrt{2\pi}} \exp\left(-\frac{\sigma^2\omega^2}{2}\right), \tag{10a}$$

$$\mathcal{F}[L] = \frac{i\omega}{\sqrt{2\pi}} \exp\left(-\sqrt{3}\sigma|\omega|\right). \tag{10b}$$

FT images of convolution of two Gaussians or two Lorentzians are the following:

$$\mathcal{F}\left[G_{\text{exp}} * G_{\text{st}}\right] = -\frac{\omega^2}{\sqrt{2\pi}} \exp\left(-\frac{\left(\sigma_{\text{exp}}^2 + \sigma_{\text{st}}^2\right)\omega^2}{2}\right), \tag{11a}$$

$$\mathcal{F}\left[L_{\text{exp}} * L_{\text{st}}\right] = -\frac{\omega^2}{\sqrt{2\pi}} \exp\left(-\sqrt{3}\left(\sigma_{\text{exp}} + \sigma_{\text{st}}\right)|\omega|\right). \tag{11b}$$

In accordance with the Fourier inversion theorem, convolution of two functions can be calculated as follows:

$$G_{\text{st}} * G_{\text{exp}}(B) = \frac{1}{\sqrt{2\pi}} \int_{-\infty}^{+\infty} \mathcal{F}\left[G_{\text{st}} * G_{\text{exp}}\right](\omega) \mathrm{e}^{iB\omega} \mathrm{d}\omega. \tag{12}$$

The maximal value of convolution function (*MaxConv*) corresponds to maximal overlapping of standard and experimental spectra ($B=0$). Hence, Eq. (12) is transformed into

$$MaxConv_{\text{G}} = \frac{1}{\sqrt{2\pi}} \int_{-\infty}^{+\infty} \mathcal{F}\left[G_{\text{st}} * G_{\text{exp}}\right](\omega) \mathrm{d}\omega. \tag{13}$$

Finally, we can draw a conclusion that the maximum value of two Gauss or two Lorentz line convolutions depends on their widths as follows:

$$MaxConv_{\text{G}}\left(\sigma_{\text{st}}, \sigma_{\text{exp}}\right) \sim \left(\sigma_{\text{st}}^2 + \sigma_{\text{exp}}^2\right)^{-\frac{3}{2}}, \tag{14a}$$

$$MaxConv_{\text{L}}\left(\sigma_{\text{st}}, \sigma_{\text{exp}}\right) \sim \left(\sigma_{\text{st}} + \sigma_{\text{exp}}\right)^{-3}. \tag{14b}$$

Taking $\alpha = \sigma_{\text{exp}}/\sigma_{\text{st}} = \Delta B_{\text{pp}}^{\text{exp}}/\Delta B_{\text{pp}}^{\text{st}}$, the deviation of the *MaxConv* parameter from its true value can be calculated as follows:

$$\text{Deviation}_{\text{G}} = \frac{MaxConv_{\text{G}}\left(\sigma_{\text{st}}, \sigma_{\text{exp}}\right)}{MaxConv_{\text{G}}\left(\sigma_{\text{st}}, \sigma_{\text{st}}\right)} - 1 = \left(\frac{1+\alpha^2}{2}\right)^{-\frac{3}{2}} - 1, \tag{15a}$$

$$\text{Deviation}_{\text{L}} = \frac{MaxConv_{\text{L}}\left(\sigma_{\text{st}}, \sigma_{\text{exp}}\right)}{MaxConv_{\text{L}}\left(\sigma_{\text{st}}, \sigma_{\text{st}}\right)} - 1 = \left(\frac{1+\alpha}{2}\right)^{-3} - 1. \tag{15b}$$

In many cases, the shape of spectral line is described by convolution of Gaussian and Lorentzian functions (Voigt profile, $V(B)$). The expression of deviation in such cases is the following:

$$\text{Deviation}_{\text{V}} = \frac{MaxConv}{MaxConv_0} - 1 = \left(\frac{1+\alpha^2}{2}\right)^{-\frac{3}{2}} \frac{f\left(\xi t/\sqrt{2}\right)}{f(t)} - 1. \tag{16}$$

Herein $t = \frac{\delta_{\text{st}}}{\sigma_{\text{st}}}$, $\xi = \frac{1+\alpha}{\sqrt{1+\alpha^2}}$ and $f(t) = \sqrt{2\pi}\exp\left(t^2\right)\text{erfc}(t)\left(2t^2+1\right) - 2\sqrt{2}t$.

It can be shown that the approximate expression can be used instead of (16):

$$\text{Deviation}_{\text{V}} = \frac{3}{2}(1-\alpha) + \bar{o}(1-\alpha). \tag{17}$$

Strict derivation of the formulae (16) and (17) is presented in Appendix 2.

On the basis of expressions (15a), (15b) and (16), we can recalculate the value of $MaxConv_{corr}$ to use it in Eq. (3) instead of $MaxConv$.

$$MaxConv_{\text{corr}} = \frac{MaxConv}{\text{Deviation} + 1}. \tag{18}$$

Figure 5 illustrates the dependence of the $MaxConv$ deviation from its expected value vs $\Delta B_{\text{pp}}^{\text{exp}}/\Delta B_{\text{pp}}^{\text{st}}$ for Gaussian and Lorentzian profiles. If the spectrum line is the Voigt function, the corresponding plot lies between Gaussian and Lorentzian functions.

As example, the influence of broadening of standard spectrum on accuracy of determining of convolution amplitude is shown in Table 2. The presented data are the results of numerical experiment with calculated triplet EPR spectra with initial line width 1.23 G. Such a width is usual for spectra of nitroxide radicals in non-degassed water solution at room temperature. Deviations in the third column were obtained by the convolution method. Deviations in the next columns were

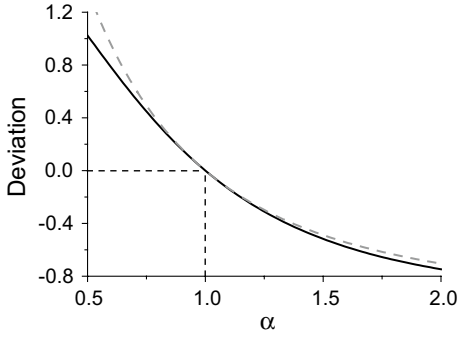

Fig. 5 Dependence of the *MaxConv* deviation from its true value vs $\alpha = \Delta B_{\text{pp}}^{\text{exp}}/\Delta B_{\text{pp}}^{\text{st}}$ for Gaussian profile (solid line) and Lorentzian profile (dash line)

Table 2 Influence of broadening of standard spectrum on accuracy in determining the convolution amplitude

Broadening of spectrum line (%)	Actual linewidth (G)	*MaxConv* deviation (%)	*MaxConv* deviation (exact correction, (16)) (%)	*MaxConv* deviation (approximate correction, (17)) (%)
0.0	1.230	0.00	0.00	0.00
2.0	1.255	− 2.95	− 2.95	− 3.00
4.0	1.279	− 5.79	− 5.79	− 6.00
6.0	1.304	− 8.52	− 8.54	− 9.00
8.0	1.328	− 11.2	− 11.2	− 12.0
10.0	1.353	− 13.7	− 13.8	− 15.0
400	6.150	− 97.0	− 97.0	–

Line shape is convolution of Gaussian and Lorentzian 1/1

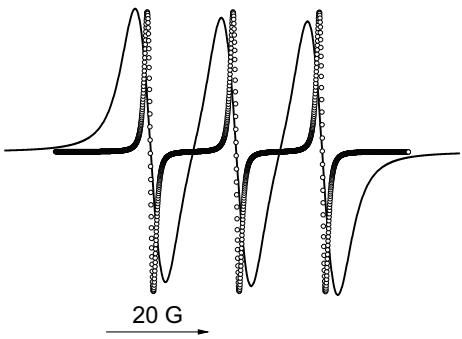

Fig. 6 Comparison of two triplet spectra with $\Delta B_{pp} = 1.23$ G (circles) and 6.15 G (line)

calculated using exact and approximate formulae (16 and 17, respectively). As seen, the approximate correction (17) is less accurate compared with the exact one (16) but it does not require information about the line shape. Comparison of the third and fourth columns demonstrates that Eq. (16) can be used even if widths of standard and experimental spectra differ by several times. Such a case is presented in Fig. 6. It should be noted that the possibility of such *MaxConv* recalculation has practical limitation. With large broadening, the individual spectral components are overlapped, so the widths of them cannot be determined accurately.

2.2.4 Test 4: The Influence of Difference in the Distances Between the Spectral Components in Experimental and Standard Spectra

In case, when the standard spectrum is obtained experimentally, some difference in the distances between the spectral components in experimental and standard spectra can be observed as a result of dependence of spin exchange interaction on concentration of paramagnetic substance. Besides, the possible way to solve the problem

of low-soluble substances (Test 2) is either to modify the solvent by adding acid or base, or to change the solvent. In such cases, the distances between the spectral components in experimental and standard spectra will also differ. We consider the simplest case, when EPR spectrum represents the several shifted lines of the identical shape (fast-motion regime) and the value of splitting (a) is much more than the line widths of components (ΔB_{pp}), so they are completely separated. For convenience, we examine here the hyperfine splitting caused by equivalent magnetic nuclei. More general case can be considered in a similar way. The FT image of a spectrum with splitting $I_{split}(B)$ is described as follows:

$$\mathcal{F}\left[I_{\text{split}}\right] = \mathcal{F}\left[I_1\right](\omega) \cdot H(\omega). \tag{19}$$

Herein, $I_1(B)$ is the shape of individual component and $H(\omega)$ describes the splitting itself. This function depends on the number and spin of magnetic nuclei. For instance, for nitroxide radicals (splitting on ^{14}N)—$H(\omega) = 1 + 2\cos(a\omega)$. As a result of calculations similar to those in Test 3, we obtain

$$\text{Deviation}_{\text{G}}^{\text{HFS}} = \frac{MaxConv_{\text{G}}\left(a_{\text{st}}, a_{\text{exp}}\right)}{MaxConv_{\text{G}}\left(a_{\text{st}}, a_{\text{st}}\right)} - 1 = \frac{2}{3}\left(\mathrm{e}^{-\theta^2}\left(1 - 2\theta^2\right) - 1\right), \tag{20a}$$

$$\begin{aligned}\text{Deviation}_{\text{L}}^{\text{HFS}} &= \frac{MaxConv_{\text{L}}\left(a_{\text{st}}, a_{\text{exp}}\right)}{MaxConv_{\text{L}}\left(a_{\text{st}}, a_{\text{st}}\right)} - 1 \\ &= \frac{2}{3}\left(\frac{\cos\left(4{*}\text{Arctan}\left(\frac{\theta}{\sqrt{3}}\right)\right) + \frac{\theta}{\sqrt{3}}\sin\left(4{*}\text{Arctan}\left(\frac{\theta}{\sqrt{3}}\right)\right)}{\left(\frac{\theta^2}{3} + 1\right)^2} - 1\right),\end{aligned} \tag{20b}$$

where $\theta = \frac{\left|a_{\text{st}} - a_{\text{exp}}\right|}{\Delta B_{\text{pp}}}$. Using Taylor series expansion, one can obtain approximate analogs of (20a) and (20b):

$$\text{Deviation}_{\text{G}}^{\text{HFS}} \sim -2\theta^2, \tag{21a}$$

$$\text{Deviation}_{\text{L}}^{\text{HFS}} \sim -\frac{4}{3}\theta^2. \tag{21b}$$

Expressions (20a, 20b) and (21a, 21b) were tested numerically on triplet spectra ($a_{\text{st}} = 16.0$ G, $\Delta B_{\text{pp}} = 1.0$ G, Gaussian and Lorentzian lines) (Table 3). One can see that exact formulae (20a) and (20b) reproduce *MaxConv* deviation. In addition, if $\theta < 0.25$ approximate expressions are applicable. Example of HFC deviation is depicted in Fig. 7.

In general, we can conclude that unlike the random error in *MaxConv* determining caused by noise, the discrepancy of line widths and distances between the spectral components of standard and experimental spectra leads to systematic errors and must be taken into account analytically. It is necessary to underline that the formulae

Table 3 Influence of the HFC deviation on accuracy of determination of the convolution amplitude

θ	a_{exp} (G)	*MaxConv* deviation (%)	*MaxConv* deviation (exact correction) (%)	*MaxConv* deviation (approximate correction) (%)
Gaussian			(20a)	(21a)
0.0	16.0	0.0	0.0	0.0
0.1	16.1	− 2.1	− 2.0	− 2.0
0.25	16.25	− 12	− 12	− 13
0.5	16.5	− 41	− 41	− 50
Lorentzian			(20b)	(21b)
0.0	16.0	0.0	0.0	0.0
0.1	16.1	− 1.3	− 1.3	− 1.3
0.25	16.25	− 7.9	− 7.9	− 8.3
0.5	16.5	− 28	− 27	− 33

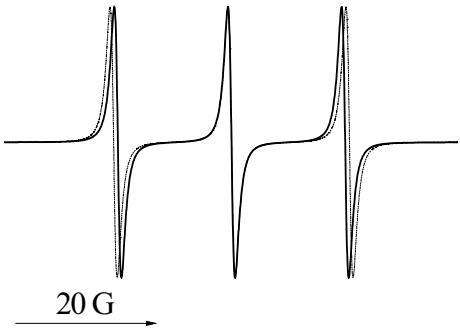

Fig. 7 Example of HFC deviation for triplet spectra. Solid line: $a = 16.0$ G, $\Delta B_{pp} = 1.0$ G, dash line: $a = 16.6$ G, $\Delta B_{pp} = 1.0$ G ($\theta = 0.6$). Both spectra have Lorentzian shape

for such a correction can be also used in case, when comparison the experimental and standard spectra are made by least-square fitting. Nevertheless, one should make efforts to obtain standard spectrum with the shape similar as possible to the shape of experimental spectra being studied.

2.2.5 Additional Notes

It should be noted that the convolution method can be applied to analysis of noisy spectra with different shapes. Maximum of convolution function of two identical spectra is observed at the point of their maximal overlapping regardless of the shape. The hyperfine structure affects the number of side maxima in convolution function. For example, convolution of two triplet spectra leads to five-component function, whereas quintet spectra result in nine-component function, etc. As an example, in Fig. 8, one can see the convolution result of theoretically calculated rigid limit EPR spectra of the typical nitroxide ($g_x = 2.0024$, $g_y = 2.0067$, $g_z = 2.0097$, $A_x = 7.2$ G, $A_y = 5.8$ G, $A_z = 34.3$ G). Autoconvolution and the convolution with artificially noised spectrum are compared. As seen, the central parts of these functions are almost identical, whereas the side parts are different. The side parts of convolution

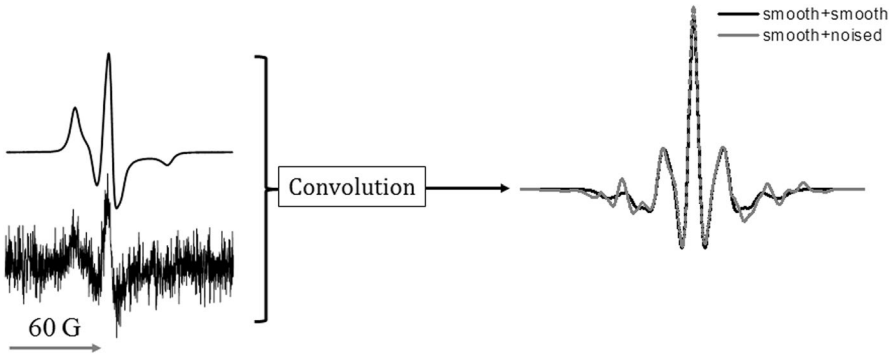

Fig. 8 Example of convolution of rigid limit EPR spectra

function correspond to overlapping and integration of the side parts of EPR spectra which are characterized by lower SNR compared with the central part.

One more problem is the influence of additional signals in experimental spectrum on the result of quantitative analysis. These may be the signals of other radicals, if the experimental sample contains the added paramagnetic substances, or signals of ampoule or resonator, which can be significant if the signal being analyzed is small. Obviously, the distortion of convolution function depends on intensity and position of additional signals in EPR spectrum. If the additional components are located in the magnetic fields outside the integration limits of convolution procedure, they do not affect the *MaxConv* value. If these components are located inside the integration limits and are not overlapped with the analyzed spectral components, and the standard spectrum is noiseless, the additional signals do not affect the result. In the same case, but provided some noise in standard spectrum, the *MaxConv* value would be increased by multiplication of additional signals by noise of standard spectrum. Note that the influence of wide additional signals is less than narrow ones because of the difference in width of thir Fourier images. All above listed will be reliable also in case when comparison of experimental and standard spectra is made by least squared fitting. As a rule, the presence of additional signals in the studied EPR spectra is highly undesirable, and the method proposed is not designed investigating such systems.

2.3 Experimental Tests

The proposed method was tested in several experimental ways. The first way is as follows. Two series of solutions of stable nitroxide radicals TEMPONE and TEMPOL in phosphate buffered saline (PBS, pH 7.4) were prepared by consecutive dilutions. EPR spectra of solutions were processed quantitatively by convolution technique and direct comparison of the spectra amplitudes with those of the standard. The amplitude measurements were performed by visual averaging of spectrum noise. It is clear that the visual averaging is quite subjective way but automatic measurements are also unreliable if the level of noise is significant. The obtained

Table 4 Results of quantitative analysis of EPR spectra of TEMPONE/PBS and TEMPOL/PBS

Real fraction	Number of scans	SNR	Fraction from convolution	Error (%)	Fraction from amplitude measurement	Error (%)
TEMPONE						
1.00	1	> 100	1.00	0	1.00	0
1.06×10^{-1}	1	~ 50	1.16×10^{-1}	9	1.19×10^{-1}	12
1.14×10^{-2}	1	2	1.32×10^{-2}	16	1.26×10^{-2}	11
1.14×10^{-2}	4	5	1.28×10^{-2}	12	1.36×10^{-2}	19
5.71×10^{-3}	1	< 1	5.93×10^{-3}	4	–	–
TEMPOL						
1.00	1	> 100	1.00	0	1.00	0
1.06×10^{-1}	1	20	1.09×10^{-1}	3	1.11×10^{-1}	5
1.12×10^{-2}	1	4	1.25×10^{-2}	12	1.40×10^{-2}	25
1.12×10^{-2}	4	7	1.23×10^{-2}	10	1.28×10^{-2}	14
2.39×10^{-3}	1	< 1	3.34×10^{-3}	40	–	–
2.39×10^{-3}	4	~ 1	2.17×10^{-3}	9	–	–

Values are calculated relatively to the most concentrated solution which contained ca. 10^{15} spins (TEMPONE/PBS) and ca. 3×10^{15} spins (TEMPOL/PBS). Dash means the impossibility of measurements. All analyzed spectra had the same line widths

values were compared with those calculated according to the dilution procedure. The results are presented in Table 4. Radicals TEMPONE and TEMPOL were chosen due to the significant difference in line widths of EPR spectra in the solution (0.4 G for TEMPONE/PBS and 1.5 G for TEMPOL/PBS). The results presented in Table 4 reveal the convolution method has some advantage compared with the direct amplitude measurement when SNR exceeds 5, but it is practically irreplaceable in

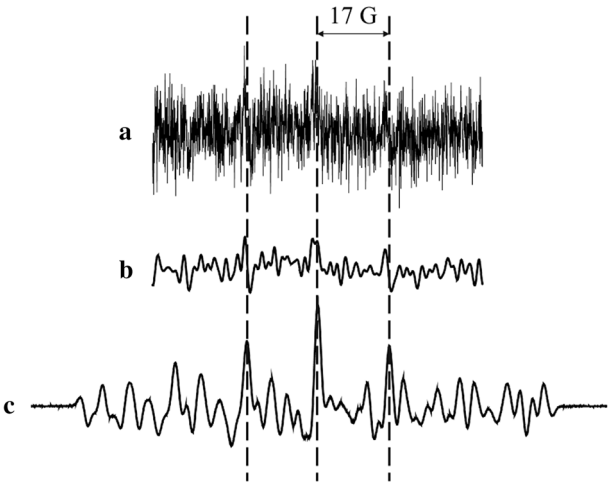

Fig. 9 Comparison of experimental EPR spectrum (a), the result of its digital denoising (b) and the result of its convolution with standard spectrum (c)

case of highly noisy spectra. It should note that in case of such noisy spectra, the reliable quantitative results cannot be received even after digital denoising procedure. As an example, Fig. 9 demonstrates the EPR spectrum corresponding to the last line in Table 4—the result of its denoising by truncation of "noise frequencies" in FT image and the result of convolution of the spectrum with the standard one.

The second experimental test was to record EPR spectra of a sample TEMPONE/PBS containing ca. 10^{13} paramagnetic molecules at different power of electromagnetic emission. Experiment was performed at power magnitudes below saturation limit which was estimated independently. Integral intensity of spectra was defined by convolution method. Obtained dependence of EPR signal intensity vs square root of power is presented in Fig. 10. As seen, the plot of the dependence is linear as it is supposed to be.

2.4 Practical Application

The convolution technique was used for the investigation of kinetic regularities of release process of the TEMPOL from biodegradable polymer (poly-D,L-lactide, PDLLA) to PBS at the temperature of 37 °C. Quantitative kinetic measurements are of great interest in connection with the great prospects of application of this polymer doped by the active pharmaceutical ingredients for medical purposes [24]. Application of paramagnetic dopants allows analyzing of not only the release but also of the processes going inside the polymer matrix during its degradation in liquid medium. Nevertheless, at the present time, there are no quantitative results concerning radical release from polylactide polymers into water solutions. The reason is the autocatalytic character of the polylactide hydrolytic degradation that is accelerated by the products of degradation (lactic acid and its oligomers). To avoid the autocatalysis, it is necessary to change PBS frequently. Therefore, it is impossible to produce large concentration of paramagnetic substance in the solution. Besides, due to the high dielectric constant of water, the size of EPR samples must be very small. As a result, the number of spins in the sample is usually low, in particular, in our experiments, it was about 1×10^{13} and

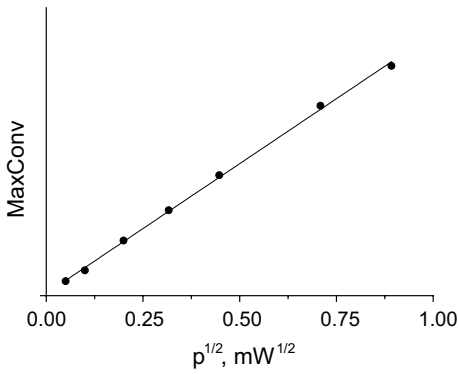

Fig. 10 Linear fragment of saturation curve received for TEMPONE/PBS sample containing ca. 10^{13} spins

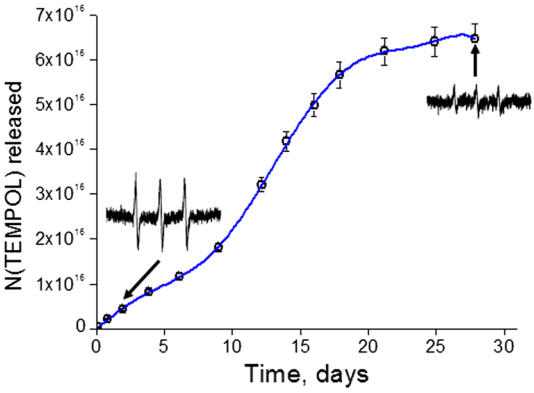

Fig. 11 Release of TEMPOL from PDLLA film into PBS at 37 °C. Quantitative data are obtained by convolution method

the spectra looked as shown in Fig. 2. These spectra were analyzed by convolution method. The experimental kinetic curve describing the TEMPOL release from PDLLA into PBS is presented in Fig. 11. As seen, the curve is very smooth; the scatter of points is small. The results obtained made it possible to investigate the release kinetics at the beginning and at the end of the process when the rate of release is low.

3 Experimental

3.1 Materials

Spin probes TEMPOL (4-hydroxy-2,2,6,6-tetramethylpiperidine-1-oxyl) and TEMPON (4-oxo-2,2,6,6-tetramethylpiperidine-1-oxyl) from Sigma-Aldrich and D,L-polylactide (RURASORB®PDL04, $M_w = 45$ kg/mol) from Purac Biochem ($T_g = 52$ °C) were used without further purification. PBS was prepared by dissolving of the standard tablet (received from the company Puschinskiye Laboratorii) in distilled water.

3.2 Sample Preparation

Solutions containing TEMPONE or TEMPOL for quantitative experiments were prepared by dissolving of solid substances in PBS and serial dilutions of the solution. The dilution procedure was controlled by weighing the solutions.

PDLLA was impregnated by TEMPOL in supercritical CO_2 using the "SCF mini-laboratory" equipment [25]. The procedure of impregnation is described in the paper [7]. The resulting foamed polymer containing paramagnetic dopant was ground into powder and then pressed (10 MPa, $T = 333$ K). As a result, a film with a thickness of 200 μm was obtained. The film fragment of 80 mm^2 was placed into 8-ml glass container and filled with 1 ml PBS. During the investigated process, the container was in a shaker at 310 K (37 °C). To control the release of TEMPOL

from PDLLA into PBS, the solution samples of 7 μl were taken during the process, and the amount of the probe in the samples was studied by EPR spectroscopy. The release curve was obtained by summation of the amount of substance released up to a certain point in time. To prevent acidification of the solution, the PBS was changed once in 1–2 days. When replacing the buffer, its weighted amount was removed and the weighted amount of fresh buffer solution was added. Based on the weight of removed and added solutions, the amount of paramagnetic substance being removed together with the solution was taken into account.

The probes of solutions for EPR spectroscopy were placed into glass tubes with inner diameter of 1.0 mm. The sample height in tube was 8–9 mm (total volume of probe is about 7 μl). EPR spectra were recorded on a Bruker EMX-500 Plus spectrometer. The high-sensitive resonator ER 4119 HS was used.

3.3 Computational Details

To perform numerical tests similar to the real experiments, the magnetic parameters of the stable nitroxide radical TEMPOL in PBS were used for simulation ($g_{iso} = 2.0057$, $A_{iso} = 17$ G).

Function that imitates the real noise in EPR spectra was added to the calculated spectra. For this purpose, the fragment of the EPR spectrum of empty resonator was recorded and the distribution function of noise intensity was determined. It was found that this function is Gaussian. Thus, for noising of the calculated spectrum, we used the algorithm generating a normally distributed random variable:

$$F(a) = \frac{1}{2}\left(1 + \mathrm{erf}\left(\frac{a}{\sigma}\right)\right). \tag{22}$$

Herein, F is a distribution function and a is a noise amplitude. SNR was defined as EPR spectrum amplitude divided by 2σ.

3.4 Software

To facilitate and unite the procedures of convolution calculation and *MaxConv* measurements, the computer program on C++ was written. The program is available free of charge at http://sourceforge.net/p/epr-convolution/.

4 Conclusions

The method of determination of number of spins from highly noisy EPR spectra is proposed. The method is based on convolution of analyzed spectrum with the spectrum of the same shape characterized by high signal-to-noise ratio (standard spectrum). Several ways to obtain the standard spectrum are discussed. Applicability of the method for quantitative processing of highly noisy EPR spectra (signal-to-noise ratio is less than 1) is shown. The method was used for the study of kinetic regularities of release of paramagnetic dopant from biodegradable polymer.

Acknowledgements This work was supported by the Russian Foundation of Basic Research (grants 14-33-00017-п, 18-29-06059, 17-02-00445) and partially by Lomonosov Moscow State University Program of Development.

Appendix 1

As an additive noise is considered, the distorted signal was calculated as follows:

$$I_{\text{exp}}(B) = I_{\text{st}}(B) + I_{\text{noise}}(B). \tag{23}$$

$I_{\text{noise}}(B)$ consists of randomly generated values in every point. In corresponding numerical tests, there is no relative shift of standard and experimental signals, so the maximum value of convolution function is at the point $B=0$.

$$MaxConv = I_{\text{exp}} * I_{\text{st}}(0). \tag{24}$$

We compared this value with another one obtained when noise is equal zero, i.e. when standard spectrum is convolved with itself ($MaxConv_0$); besides, we calculated the relative deviation of *MaxConv* (*Dev*):

$$MaxConv_0 = I_{\text{st}} * I_{\text{st}}(0), \tag{25}$$

$$\begin{aligned} Dev &= \frac{MaxConv - MaxConv_0}{MaxConv_0} = \frac{I_{\text{exp}} * I_{\text{st}}(0)}{I_{\text{st}} * I_{\text{st}}(0)} - 1 \\ &= \frac{I_{\text{st}} * I_{\text{st}}(0) + I_{\text{noise}} * I_{\text{st}}(0)}{I_{\text{st}} * I_{\text{st}}(0)} - 1 = \frac{I_{\text{noise}} * I_{\text{st}}(0)}{I_{\text{st}} * I_{\text{st}}(0)}. \end{aligned} \tag{26}$$

As follows from Eq. (26), the value of *Dev* is different for different functions of $I_{\text{noise}}(B)$, i.e. for different noise scattering along the spectrum. For example, the structure of noise is not changed, if I_{noise} is multiplied by (− 1) and in agreement with Eq. (2), *Dev* also inverses its sign. The latter means that the mathematical expectation of *Dev* can be zero.

In the real experiment, the point $B=0$ cannot be determined exactly. In such a case, the maximal value of convolution function is taken as *MaxConv.* This leads to a slight shift of mathematical expectation of *Dev* to a positive area. Figure 12 presents the *MaxConv* deviation in the first numerical experiment (triplet spectrum, $a=17$ G, $\Delta B_{\text{pp}}=1.5$ G 2000 tries of noising) for SNR 20 (a) and 0.5 (b) with automatically measurement of *MaxConv* as a maximum of convolution function.

Appendix 2: Dependence of *MaxConv* Deviation vs Broadening of EPR Spectra

In the text above, we discussed the deviation of calculated *MaxConv* from its true value, if the linewidths of standard and experimental spectra are not coincided. Gaussian and Lorentzian profiles were considered. In many cases, line shapes are the convolution of Gaussian and Lorentzian functions [Voigt profile, $V(B)$]. Therefore, the Voigt profile is

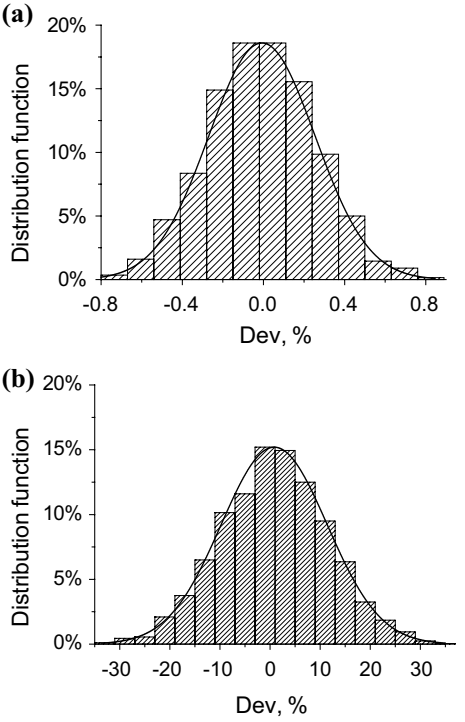

Fig. 12 Distributions of *MaxConv* deviation in numerical experiment (2000 attempts of noising) for SNR 20 (**a**) and 0.5 (**b**) and their fitting with Gaussians

characterized by two parameters which are denoted here as σ_G and σ_L. These parameters reflect the Gaussian and Lorentzian contribution to the line shape. In this appendix, the deviation of *MaxConv* in case of Voigt profile is considered.

Fourier-transform image of Voigt profile can be written in agreement with convolution theorem:

$$\mathcal{F}\left[V_{\sigma_G,\sigma_L}\right] = \frac{i\omega}{\sqrt{2\pi}} \exp\left(-\frac{\sigma_G^2\omega^2}{2}\right) \exp\left(-\sqrt{3}\sigma_L|\omega|\right). \tag{27}$$

For convenience, we change the designation. Further, we put $\sigma = \sigma_G$, $\delta = \sqrt{3}\sigma_L$. Hence, the convolution of two Voigt profiles is as follows:

$$\mathcal{F}\left[V_{exp} * V_{st}\right] = -\frac{\omega^2}{\sqrt{2\pi}} \exp\left(-\frac{\left[\sigma_{st}^2 + \sigma_{exp}^2\right]\omega^2}{2}\right) \exp\left(-\left[\delta_{st} + \delta_{exp}\right]|\omega|\right), \tag{28}$$

$$MaxConv = \int_{-\infty}^{+\infty} \mathcal{F}\left[V_{exp} * V_{st}\right] d\omega = \frac{\exp\left(-\frac{\Delta^2}{2\Sigma^2}\right)\left(\Delta^2 + \Sigma^2\right)\mathrm{erfc}\left(\frac{\Delta}{\sqrt{2\Sigma^2}}\right) - \sqrt{2/\pi}\Sigma\Delta}{\Sigma^5}, \tag{29}$$

where $\Delta = \delta_{st} + \delta_{exp}$, $\Sigma^2 = \sigma_{st}^2 + \sigma_{exp}^2$.

If the line shape is not changed with broadening, i.e. Gaussian and Lorentzian contribution to the Voigt profile remains the same, we can take $\alpha = \delta_{exp}/\delta_{st} = \sigma_{exp}/\sigma_{st} = \Delta B_{pp}^{exp}/\Delta B_{pp}^{st}$.. Finally, the expression of the *MaxConv* deviation can be deduced:

$$\text{Deviation}_V = \frac{MaxConv}{MaxConv_0} - 1 = \left(\frac{1+\alpha^2}{2}\right)^{-\frac{3}{2}} \frac{f\left(\xi t/\sqrt{2}\right)}{f(t)} - 1. \quad \text{(30, 16 in the main text)}$$

Herein $t = \frac{\delta_{st}}{\sigma_{st}}$, $\xi = \frac{1+\alpha}{\sqrt{1+\alpha^2}}$ and $f(t) = \sqrt{2\pi}\exp\left(t^2\right)\text{erfc}(t)\left(2t^2+1\right) - 2\sqrt{2}t$. Note, that the parameter t points out the contribution of components to the Voigt profile, e.g. $t=0$ is regarded as the Gaussian case and $t = \infty$ as the Lorentzian one. Analysis of Eq. (30) is rather complicated but it can be found (at least, graphically) that for any α (hence, for any fixed broadening) Deviation_V is the monotonic function of parameter t and is changed from Gaussian limit (15a) to Lorentzian one (15b). Moreover, for any t (that means for any Voigt profile):

$$\text{Deviation}_V = \frac{3}{2}(1-\alpha) + (1-\alpha). \quad \text{(31, 17 in the main text)}$$

One can use the first summand only with the minimum error for α in the range [0.83, 1.20]. It should be noted that it is not always possible to estimate the parameters σ_G and σ_L in experiments. However, if $\alpha > 1$, the difference between Gauss and Lorentz corrections is far less than the error of Q-factor measurement. This means that the formula (15a) or (15b) is acceptable in case of Voigt profile.

References

1. J.E. Wertz, J.R. Bolton, *Electron Spin Resonance* (Elementary Theory and Practical Applications. McGraw Hill Book Co., New York, 1972)
2. A.N. Kuznetsov, *The Method of Spin Probes* (Nauka, Moscow, 1976)
3. L.J. Berliner (ed.), *Spin Labeling. Theory and Applications* (Academic Press, New York, 1976)
4. G.I. Likhtenshtein, *The Method of Spin Labels in Molecular Biology* (Nauka, Moscow, 1974)
5. M. Drescher, G. Jeschke (eds.), *EPR Spectroscopy: Applications in Chemistry and Biology* (Springer, Heidelberg, New York, 2012)
6. G.R. Eaton, S.S. Eaton, D.P. Barr, R.T. Weber, *Quantitative EPR* (Springer, Vienna, 2010)
7. N.A. Chumakova, T.A. Ivanova, E.N. Golubeva, A.I. Kokorin, T Appl. Magn. Reson. **49**, 511–522 (2018)
8. M. Srivastava, C.L. Anderson, J.H. Freed, IEEE Access **4**, 3862–3877 (2016)
9. ChE Cook, M. Bernfeld, *Radar Signals* (Academic Press, New York, London, 1967)
10. M.I. Skolnik, *Radar Handbook* (McGraw-Hill, Boston, 1990)
11. G.A. Korn, T.M. Korn, *Mathematical Handbook* (Nauka, Moscow, 1984)
12. A.I. Smirnov, R.L. Belford, J. Magn. Reson. A **190**, 65–73 (1995)
13. D.R. Duling, J. Magn. Reson. B **104**, 105–110 (1994)
14. W.R. Dunham, J.A. Fee, L.J. Harding, H.J. Grande, J. Magn. Reson. **40**, 351–359 (1980)
15. N.D. Yordanov, Appl. Magn. Reson. **6**, 241–257 (1994)
16. N.D. Yordanov, M. Ivanova, Appl. Magn. Reson. **6**, 333–340 (1994)

17. A.Kh. Vorobiev, N.A. Chumakova, in *Nitroxides Theory, Experiment and Applications*, ed. by A.I. Kokorin (INTECH, Rijeka, 2012), pp. 57–112
18. D.J. Schneider, J.H. Freed, in *Biological Magnetic Resonance*, vol. 8, ed. by L.J. Berliner, J. Reuben (Plenum, New York, 1989), pp. 1–76
19. D.A. Chernova, A.Kh. Vorobiev, J. Appl. Polym. Sci. **121**, 102–110 (2011)
20. D.A. Chernova, A.K. Vorobiev, J. Polym. Sci. Part B Polym. Phys. **47**(2009), 107–120 (2009)
21. Yu.N. Molin, K.M. Salikhov, K.I. Zamaraev, *Spin Exchange* (Springer-Verlag, Berlin, New York, 1980)
22. K.M. Salikhov, Appl. Magn. Reson. **38**, 237–256 (2010)
23. B.Y. Mladenova, N.A. Chumakova, V.I. Pergushov, A.I. Kokorin, G. Grampp, D.R. Kattnig, J. Phys. Chem. B **116**, 12295–12305 (2012)
24. M. Santoro, S.R. Shah, J.L. Walker, A.G. Mikos, Adv. Drug Deliv. Rev. **107**, 206–212 (2016)
25. N.V. Minaev, Patent registration number 147199, Russia (2014)